# A-Band shortening in single fibers of frog skeletal muscle

Ammasi Periasamy, David H. Burns, Dale N. Holdren, Gerald H. Pollack, and Karoly Trombitás
Center for Bioengineering WD-12, University of Washington, Seattle, Washington 98195

ABSTRACT The question of whether A-bands shorten during contraction was investigated using two methods: high-resolution polarization microscopy and electron microscopy. During shortening from extended sarcomere lengths in the passive state, sarcomere-length changes were essentially accounted for by I-band shortening. During active shortening under otherwise identical conditions, the sarcomere length change was taken up approximately equally by A- and I-bands. Several potential artifacts that could give rise to apparent A-band shortening were considered and judged unlikely. Results obtained with polarization microscopy were similar to those obtained with electron microscopy. Thus, modest but significant thick filament shortening appears to occur during active sarcomere shortening under physiological conditions.

## INTRODUCTION

Although the constancy of thick filament length has become implicit in current thinking about muscle, the number of reported exceptions has been surprisingly large (for review, see Pollack, 1983, pp. 1052–1066). Many of these studies, on the other hand, were conducted in a cursory manner and under conditions outside the physiological range. This prompted us to reinvestigate the question, especially in light of the fundamental significance of the issue.

The most comprehensive study of A-band widths in living muscle was carried out more than 30 years ago by Huxley and Niedergerke (1954, 1958). Below natural length, A-band shortening was found consistently during contraction, but was attributed to the limited resolution of their optical system. Above natural length, A-band width remained approximately constant, especially at the upper end of the physiological sarcomere length range, but equipment available at the time imposed restrictions upon both spatial and temporal resolution.

To reinvestigate the question with improved resolution, we made use of the high numerical aperture optics now available, as well as modern digital image processing methods. Further, we were able to check our observations by conducting parallel studies using the electron microscope. The results confirm the Huxley/Niedergerke observation that the A-band width does not change above natural length under passive conditions, but in activated fibers we found consistent A-band shortening.

Dr. Periasamy's current address is Dept. of Cell Biology and Anatomy, University of North Carolina, Chapel Hill, NC 27599.

## METHODS

### Video polarizing microscopy

It is well known that with ordinary light microscopy, distinction of A-and I-bands can be ambiguous. Interference and polarization microscopy, on the other hand, allow certainty in designating band assignments (Huxley and Niedergerke, 1958). Interference microscopy is difficult to perform correctly, requiring close matching of the refractive indices of solution and muscle, with consequent questions as to the effect of the matching substance on fiber behavior. To avoid any such uncertainty, polarizing microscopy was used. In this technique, contrast is based on birefringence and is thus dependent upon the packing of protein filaments as well as the intrinsic properties of the proteins themselves. Highly birefringent A-band regions appear bright, while less birefringent I-band regions and the background are dark. Background darkness can be used to confirm unambiguously the distinction of A- and I-bands.

The microscope used in our study was originally constructed by Prof. Shinya Inoué, although several modifications were made. The optical layout is shown in Fig. 1. Light emitted from a 75-W pulsed xenon arc lamp (Strobex Model 136, Chadwick-Helmuth, Monrovia, CA) was collected and filtered with a set of bandpass filters, limiting the wavelength passband to 565 ± 15 nm. Pulse duration was set at 25 $\mu$s, and pulses were triggered using the 60-Hz sync signal from the video camera. An infrared reflecting filter was used to filter higher order wavelengths and to ensure minimal heating of the sample. The nearly monochromatic light was polarized by a goniometer-mounted, Glan-Thompson high-extinction calcite prism, acting with a mica ¼ wave plate to provide Sénarmant compensation. A strain-free condenser (N.A. 1.4; Carl Zeiss, Inc., Thornwood, NY) illuminated the sample using Köhler illumination. This condenser was equipped with a rectifier (Nikon, Tokyo, Japan) to minimize any polarization change induced by the optics. The addition of this component makes possible the use of large numerical apertures not practical before its relatively recent introduction. Images were collected using a hand-selected strain-free objective (N.A. 1.25, 97×, American Optical, Framingham, MA) and a second fixed Glan-Thompson prism acting as a analyzer. The resulting image was then projected onto a vidicon camera.

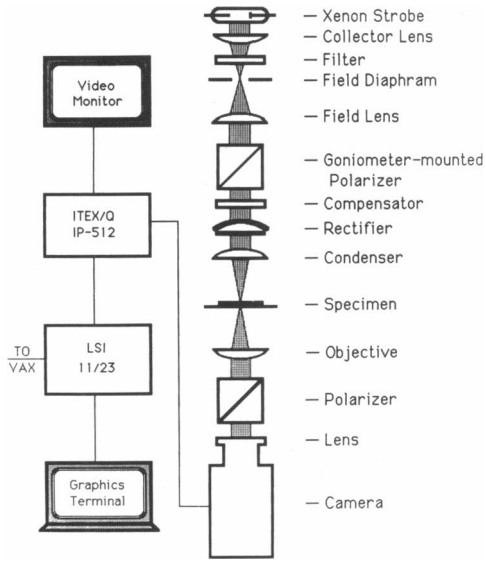


FIGURE 1 Schematic of polarizing microscope (*right*) and associated image processing system (*left*). See text for details.

## Image collection

A 1" silicon target vidicon camera (RCA TC-1500/U; RCA, Lancaster, PA) was chosen as detector because of its high resolution and low lag. The automatic gain of the camera was eliminated, and a fixed gain was substituted. Likewise, a constant black level reference was provided by blocking light from the bottom 20% of the vidicon target. To ensure the same $x$- and $y$-axis magnification, the vertical sweep of the camera was fine-adjusted to provide an aspect ratio of 1:1. This was accomplished by imaging a grid target with a high-resolution lens (50 mm, f/# 1.8, Nikon). Geometric distortion of the camera was found to be <0.5% over the entire field.

Video output from the camera was digitized by connecting the camera to an image processing module (model IP-512, Imaging Technology, Woburn, MA) that contained a flash analog-to-digital converter operating at 10 MHz with eight-bit resolution. The digital values were stored in either one of two 512 × 512 pixel frame buffers, internal to the IP-512 system. One frame buffer was configured as eight bits deep for general image collection, while the other was 16 bits deep, thereby allowing image summing and storage. The image digitizing system allows complete 512 × 480 pixel images to be collected in 1/30 s. However, because the system operated using an interlace of two separate fields taken 1/60 s apart, alternate rows of the image were separated by 1/60 s. To avoid consequent jitter induced by fiber motion and potential artifacts therefrom, images were analyzed as two separate 512 × 240 frames. The IP-512 system was interfaced to a LSI-11/23 (DEC; Maynard, MA) computer, and could be addressed through a series of internal registers in that computer.

We developed a software package for the LSI-11/23 to perform various manipulations of the images stored in the frame buffers. The program could freeze a frame or store and retrieve from a hard disk any portion of a digitized image. For fast acquisition of frames, a routine was written that stored a selected strip of the full 512 × 480 image in the 16-bit frame buffer. This avoided the time-consuming (≈14 s) task of storage to hard disk between successive image acquisitions, and allowed 50-row frame segments to be stored at a rate of 5 Hz/frame segment. Thus, several frame segments in succession could be obtained during a single contraction.

Finally, geometric calibration of the video microscope system was accomplished by imaging a series of gratings with known period (American Holographic, Acton, MA). The spacing of the grating images could then be compared to a computer-generated grid, also of known period. In this manner, pixel spacing for the $x$ and $y$ axes was found to correspond to 0.054 $\mu$m on the image. By observing the alignment of the grid with the grating image, the pixel spacing was confirmed to be uniform within two pixels over the full frame.

Resolution of the optical system, calculated by the Rayleigh criterion, was nominally 268 nm. We measured resolution directly, using a thin (100 nm) chromium-edge object in the object plane of the microscope. The microscope point-spread function is the derivative of the image of this "step" object. We placed the edge object at several positions and orientations in the field and measured the point-spread function. Typically, the half-width, and thus the resolution, was 350 nm, slightly poorer than the nominal resolution.

## Digital image processing

With the images in digital form, various image-processing algorithms could be applied to enhance the contrast and thus resolution between A- and I-bands. When a vidicon detector is used, pixel sensitivity across the photosensitive surface varies due to a change in efficiency with angle of the scanning electron beam. The effect is characterized as maximum brightness of the image at the center of the frame with a general dimming near the frame edges. To reduce the nonuniformities in both illumination and detector sensitivity we referenced each image to an image without an object present, taken from a region next to the fiber. For the background image, the polarizer was rotated to allow sufficient illumination for accurate measurements. A ratio of this frame to subsequent striation images allowed a substantial reduction in background nonuniformity. The effect of this background-correction procedure can be seen in Fig. 2, *a* and *b*. Contrast between the light and dark regions in the image is enhanced, and the overly dark region at the left is lightened. For improved visualization, the gray scale seen in Fig. 2 *b* was adjusted to fill the entire 256 gray levels that can be displayed by the system. The result is shown in Fig. 2 *c*. This expansion merely allows better visualization, but does not affect data in any manner.

In pilot experiments, we also implemented each of several digital deconvolution approaches to attempt to compensate for the microscope's limited optical bandwidth. Several algorithms were developed, including Wiener filtering and maximum entropy deconvolution. Although some image improvement was realized, we judged the improvement modest relative to the uncertain effect on band measurements that might be introduced by such filtering, in light of the influence of objects outside the focal plane. Therefore, we chose not to implement these algorithms in this study.

## Signal averaging

Because the desired information is uniaxial, pixels perpendicular to this axis can be summed together. The original two dimensional image is thus reduced to a one-dimensional densitometric trace with random noise averaged out. For the sum to represent a faithful description of the original image, skew of the striations must be minimal. Though care was always taken to restrict observations to regions with minimal skew, some skewing was generally unavoidable, particularly during contraction. Therefore, an automated procedure for skew reduction was developed. With one arbitrary densitometric trace as a standard, a cross-correlation algorithm was used to find the axial offset of each subsequent trace that produced best alignment with the standard. An example of the skew

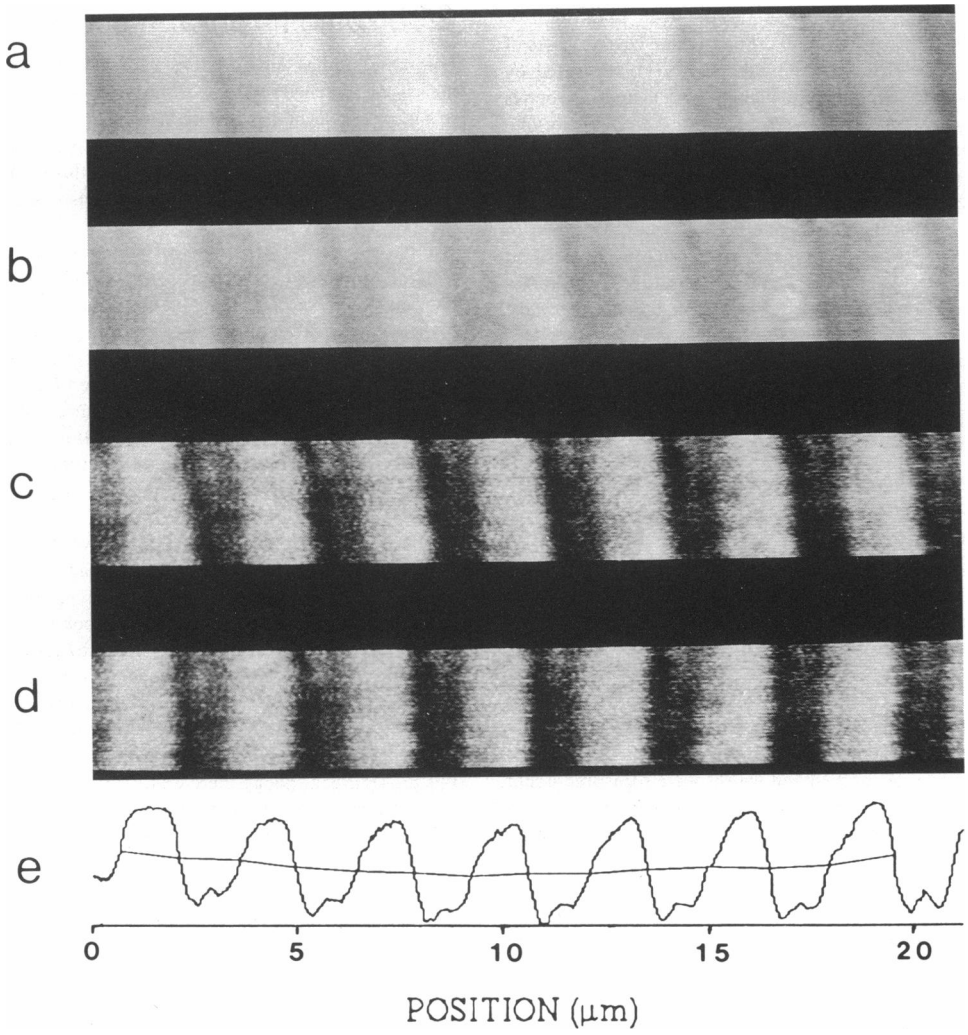


FIGURE 2 Example of stages of image processing. A-bands bright, I-bands dark. (*a*) Raw image obtained from relaxed fiber, sarcomere length 2.94 μm; (*b*) after correction for background nonuniformity; (*c*) after gray-scale expansion; (*d*) after de-skewing of striations; and (*e*) resultant densitometer trace: average of densitometer scans across entire frame. Intersections of jagged line and densitometer trace denote computed A/I boundaries.

reduction for the image in Fig. 2 *c* is shown in Fig. 2 *d*. The skew-corrected image could now be summed in a direction perpendicular to the fiber axis without blurring of the A/I boundaries. This procedure greatly increased the signal-to-noise ratio of the densitometric traces.

## Band measurement

For measurement of A- and I-bandwidths, we followed the procedure used by Huxley and Niedergerke (1958). By band "width" we refer to the dimension along the fiber axis. Local maximas and minimas of the densitometric trace were determined. Each 50% point between an adjacent local maximum and minimum was considered an A-I boundary. Distance between successive boundaries was thus equivalent to the corresponding A- and I-band widths. The determined A-and I-band regions are shown in Fig. 2 *e*. In addition to this 50% criterion, we checked our results using 30% and 70% criteria (see Results).

## Fiber preparation and mounting

Using cornea scissors and ultrafine forceps, single fibers were isolated from toe muscles (*lumbricalis digitorum IV*) of the frog *Rana temporaria*. Dissections were carried out at room temperature in a petri dish containing a thin layer of silicone elastomer at the bottom (Sylgard, Dow Corning Corp., Midland, MI), and a physiological salt solution (in millimolar) NaCl, 115.5; KCl, 2.0; $NaH_2PO_4$, 0.20; $CaCl_2$, 1.8; $Na_2HPO_4$, 2.30; pH 7.4. Fiber viability was tested by observing the quality of fiber twitches initiated by a low-current stimulator. Slack length was 1–2 mm, while fiber diameter was 25–40 μm.

A hole was punched in each tendon, and the fiber was mounted horizontally in a chamber between two stainless steel needles. One of the needles was attached to a piezoelectric bilayer (Vernitron Piezoelectric, Bedford, OH), which bends in response to an input voltage. The other needle was fixed. This allowed us to stretch and release one end of the fiber at various rates over a wide range of sarcomere lengths. Platinum

wire electrodes were centered on either side of the fiber. Both the floor and the roof of the chamber were made of microscope cover glasses of thickness ~125 μm (Erie Scientific, Portsmouth, NH), separated by ~475 μm, small enough to accommodate high numerical aperture optics with limited working distance. Silicone vacuum grease (Dow Corning Corp.) was applied at the edges of the coverglass to avoid leakage of the solution. The entire chamber was then placed on the microscope stage with the fiber oriented at 45° to the plane of polarization.

The compactness of the chamber made it technically awkward to install a suitable tension transducer; therefore, tension was measured separately under comparable conditions in another setup (cf. Granzier and Pollack, 1985). For the slower release rate (0.1 lengths per second), the tension was ~50% of isometric; for the faster rate (0.5 lengths per second) tension was reduced to several percent isometric.

## Experimental procedures

Experiments were carried out at room temperature, as in the earlier experiments of Huxley and Niedergerke. Rectangular pulses of 1 ms duration were delivered at 33 Hz from a stimulator (model SMD9, Grass Instrument Co., Quincy, MA) to produce a tetanus with only slight ripple ~10% of maximal tetanic tension. Higher frequencies shortened the fibers' life span. Stimulus strength was set to ~10% above threshold. Tetanus duration was ~3 s. In several experiments the stimulus frequency was raised from 33 to 100 Hz, and the results appeared indistinguishable. In all experiments, fibers were allowed to rest a minimum of 4-min intervals between stimulation. Data were not used if the threshold value changed during the experiment.

For unstimulated fibers, A- and I-band widths were measured under two protocols. In the "static" protocol, the specimen was merely stretched or released to each of various sarcomere lengths ranging between 2.2 and 3.4 μm. After a short stabilization period, the image was recorded. The order of sarcomere lengths was randomized. In the "dynamic" protocol, the specimen was initially stretched to a sarcomere length of ~3.2 μm. It was then released at 0.1 length per second (one of the speeds used in the activated fibers) for 3 s, at which time it had reached a sarcomere length slightly above 2 μm. Images were recorded at varying times during release.

For measurements in tetanically stimulated fibers, the activated specimen was released at the onset of stimulation from an initial sarcomere length of ~3.2 μm at either of two velocities: 0.1 or 0.5 lengths per second. These velocities were chosen to give tensions, relative to isometric, that were approximately half-maximal, and nearly unloaded, respectively. Several regions of each fiber were interrogated, and the order of measurement was randomized.

The striation patterns were recorded for both passive and active fibers in two ways: in early experiments we captured full frames, 512 × 480 pixels. This was done before release and at some time during the release. Because of computer limitations on the data-collection rate, only one frame per contraction could be recorded. In later experiments this was ameliorated by storing only "strips" of the original frame, either 50 or 100 rows by 512 pixels. With this recording method, we could obtain samples every 100 or 200 ms, respectively, throughout the same contraction. Timing of exposures relative to the stimulus was controlled by a clock.

Subsequent to the experiment, regions of each frame or strip were selected for analysis. Selection was based solely on striation clarity: regions or entire frames were rejected if they were noisy, blurred, or excessively skewed, or if the fiber had translated out of the optical field. No additional selection criteria were imposed. Generally, zero to two frames per contraction (or release) satisfied these criteria. Thus, 16 fibers were included in the optical microscope section. Seven additional fibers were used in the electron microscope section.

## Electron micrographic studies

For these studies, single fibers were mounted between two platinum hooks, one attached to a force transducer (Akers, AME 801E), the other to a moveable lever arm, whose load could be adjusted between 0 and 50 mg. The platinum hooks served both as supports and as stimulating electrodes. All conditions, including stimulus parameters, bathing solution, and temperature, were similar to those used in the optical experiments.

First, isometric tetanic tension was measured at rest length. Fibers generally produced stable tension plateaus of 20–25 mg, depending on fiber diameter. Specimens unable to produce a stable tension plateau for 3 s were discarded. (Fibers were not tested to distinguish fast [twitch] from slow [tonus] fibers, because twitch fibers predominate, and such tests can degrade subsequent performance.) Fibers were then preloaded with 5–7 mg, such that their length increased by 30–40%, thereby increasing mean sarcomere length to ~3.0 μm. An afterload was set at 10–20 mg, high enough to offer substantial load, but low enough to permit substantial active shortening. An adjustable stop was set to limit shortening.

Specimens were then elevated just above the solution-filled chamber, stimulated tetanically, allowed to shorten against the afterload and up to the stop, then immediately reimmersed in the chamber which now contained fixative. The entire procedure took 15–20 s. The specimen was held in the mechanical apparatus and stimulated not only during this procedure, but also during subsequent fixation. Either of two types of fixative were used: mercuric chloride in alcohol and chloroform (Brown and Hill, 1982); and 2.5% glutaraldehyde in $K^+$-Ringer's solution ($Na^+$ was replaced by $K^+$). In both instances tension was maintained during this procedure: although there was a very gradual tension diminution, at least 50% of tetanic tension remained after 30 min isometric fixation. Fibers were then removed from the apparatus, stained with 2% uranyl acetate in ethanol, and embedded in Araldite.

Sections were cut with knife edge parallel to the fiber axis. They were post-stained with potassium permanganate and lead citrate, and examined in a Philips 420 electron microscope (Philips Electronic Instruments, Inc., Mahwah, NJ). Magnifications were calibrated at least once per session, using a Pt/C replica of a calibration grating ($d$ = 463 nm). The grating was inserted into the microscope and focused by adjusting its vertical position. In this way possible magnification errors arising out of lens hysteresis were avoided.

During photographic printing, all negatives including that of the calibration grating were printed with the enlarger kept at the same setting. Measurements were made from sarcomeres near the center of the field to avoid errors arising out of barrel or pincushion distortion.

# RESULTS

## Unstimulated fibers

Experiments with unstimulated fibers were carried out principally as a control, to test whether previously documented changes in A- and I-band widths in the relaxed fiber could be reproduced here. Fig. 3 *A* shows a series of representative striation patterns recorded during the "dynamic" release protocol. The same photographic exposure was used for each. The principal bands could be readily distinguished from one another. In these polarization images, the strongly birefringent A-band appears bright, while the weakly birefringent I-band is dark. In some fibers, the striation pattern became progressively more

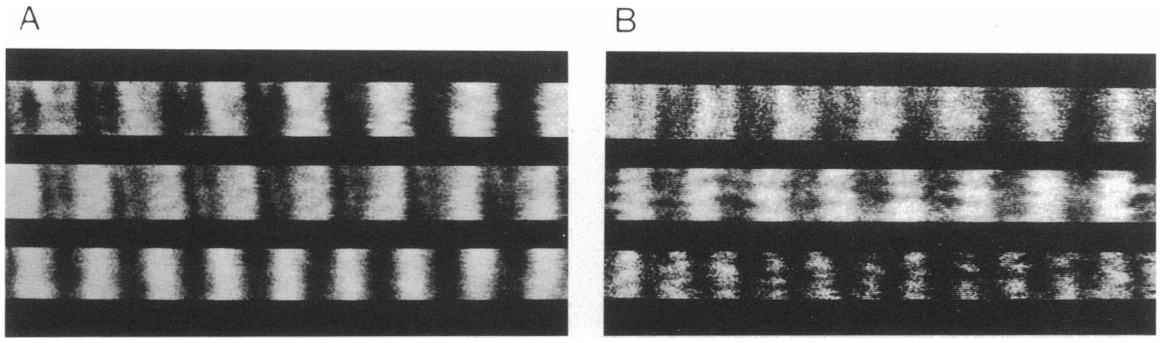


FIGURE 3 Striated images obtained during passive retraction (*A*) and active shortening (*B*). In each sequence, records at three different degrees of shortening are shown (top to bottom). A-bands bright, I-bands dark. All records have been de-skewed. M- and Z-lines are visible in some panels.

irregular as the fiber was stretched beyond a sarcomere length of ~3.0 μm; the bands often took a zigzag course across the fiber. These skewed bands could be well straightened using the anti-skewing algorithm.

Fig. 4 *A* shows that the measured width of the A-band generally remained near 1.4–1.5 μm, whereas the width of the I-band decreased linearly with decreasing sarcomere length. The slight decrease (~10%) in A-band width and decreasing sarcomere length over the same range was also observed in our earlier study involving skinned fibers (Periasamy et al., 1985). Almost the entire change in sarcomere length took place in the I-bands, as has been

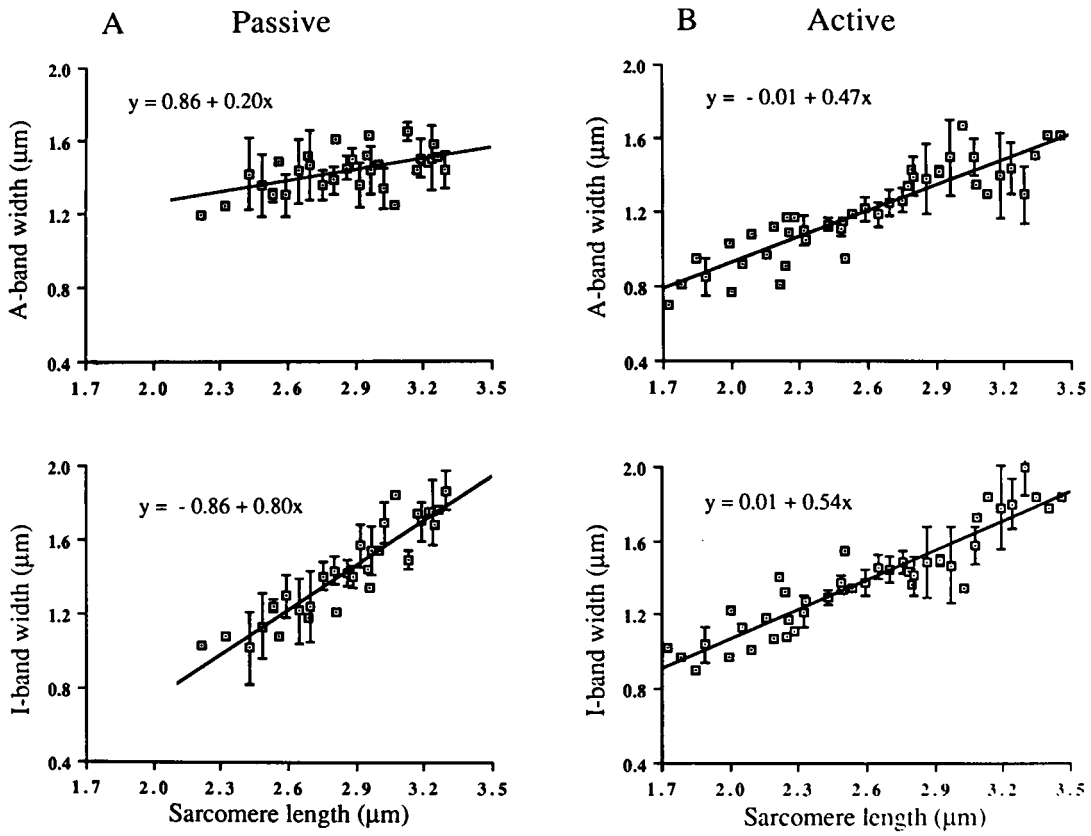


FIGURE 4 Variations in A- and I-band widths during passive (*A*) and active (*B*) shortening from long sarcomere length. Error bars denote standard deviation. Regression lines given. Number of data points: (*A*) 100; (*B*) 91.

previously found (Huxley and Niedergerke, 1954, 1958). Results obtained with the "static" protocol (not shown) were indistinguishable within experimental error.

## Activated fibers

In these experiments, the fiber was released at the onset of contraction. Fig. 5 shows a representative trace of tetanic tension, both isometric (*A*) and during isovelocity release (*B*). Isometric tetani were relatively flat with some creep, whereas tension during release tended to decline after having reached a peak. The decline is related at least in part to the progressive decrease of passive force as the fiber shortens (compare tension baselines before and after contraction); it may also arise from shortening-induced deactivation (Edman, 1975), and possibly also from fatigue, though the plateau did not wane during isometric tetani of comparable duration. Sarcomere length traces were obtained from localized regions by laser diffraction (Granzier and Pollack, 1985). Local changes of sarcomere length were frequently observed during isometric tetani, as shown on the upper panel; generally, these sarcomere lengths attained some quasi-stable value. During the isovelocity release, sarcomeres shortened in roughly a ramplike manner.

Fig. 3 *B* shows representative striation images obtained during activated shortening. Note that the light (*A*) and dark (*I*) bands both decrease with shortening. Fig. 4 *B* shows that the decrease was comparable in magnitude in each band.

To determine whether the apparent A-band shortening seen during active contraction was significant, data were analyzed statistically. Each data set was fit with a regression line; see respective panels of Fig. 4. We then computed the ±2 SD bounds along each regression line and compared passive and active shortening. Bounded regions no longer overlapped as the sarcomere shortened to 2.9 μm and below. At 2.9 μm, in other words, A-band width difference was significant at the 95% confidence level; at shorter sarcomere lengths the confidence level grew considerably.

On the other hand, such statistics apply only if the linear regression properly characterizes the data; a better fit may require something more complex than a straight line. Nevertheless, the difference between passive and active A-band widths remained unambiguous below ~2.6 μm: below this sarcomere length active and passive data points did not overlap, without exception. Thus, irrespective of analytical procedure, the A-band width decrease during active shortening was apparent at least over a limited sarcomere length range.

The data of Fig. 4 include those from both fast (0.5 lengths per second) and slow (0.1 lengths per second) release. To ascertain whether the speed of release (and hence the load) had any serious effect on the results, we plotted the data separately. Fig. 6 shows that little or no difference between the data sets could be discerned. The only obvious difference is that the extent of sarcomere shortening was higher when the load was lighter, i.e., when the release occurred at higher speed. However, the functional relations between sarcomere shortening and A-band shortening remained similar.

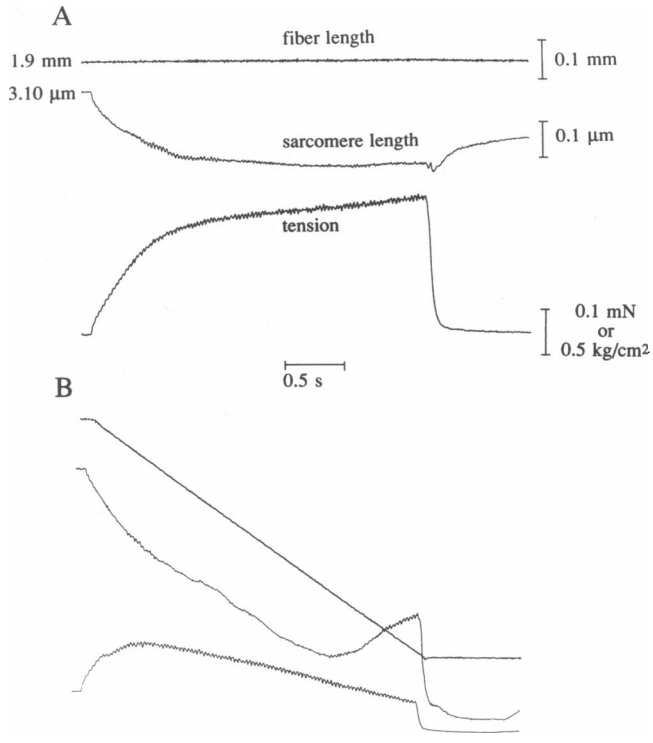


FIGURE 5 Mechanical data from representative fiber. (*A*) time course of tension development and local sarcomere-length change during isometric tetanus; (*B*) the same during isovelocity release. Scales similar for two sets of records.

## Effect of criterion

Because we cannot be certain how molecular structure translates to optical image, the choice of a criterion for the boundary between A- and I-bands is necessarily arbitrary. Detailed modeling studies will be required to determine whether the 50% intensity criterion, or perhaps some other criterion, most closely reflects the location of the edge of the thick filament array. For example, birefringence variations along either one of the two bands may be introduced during activation (Eberstein and Rosenfalck, 1963); this may shift the 50% point away from the thick filament boundary. Unless the nature of any such variations is known exactly, it is not possible to track the boundary with confidence.

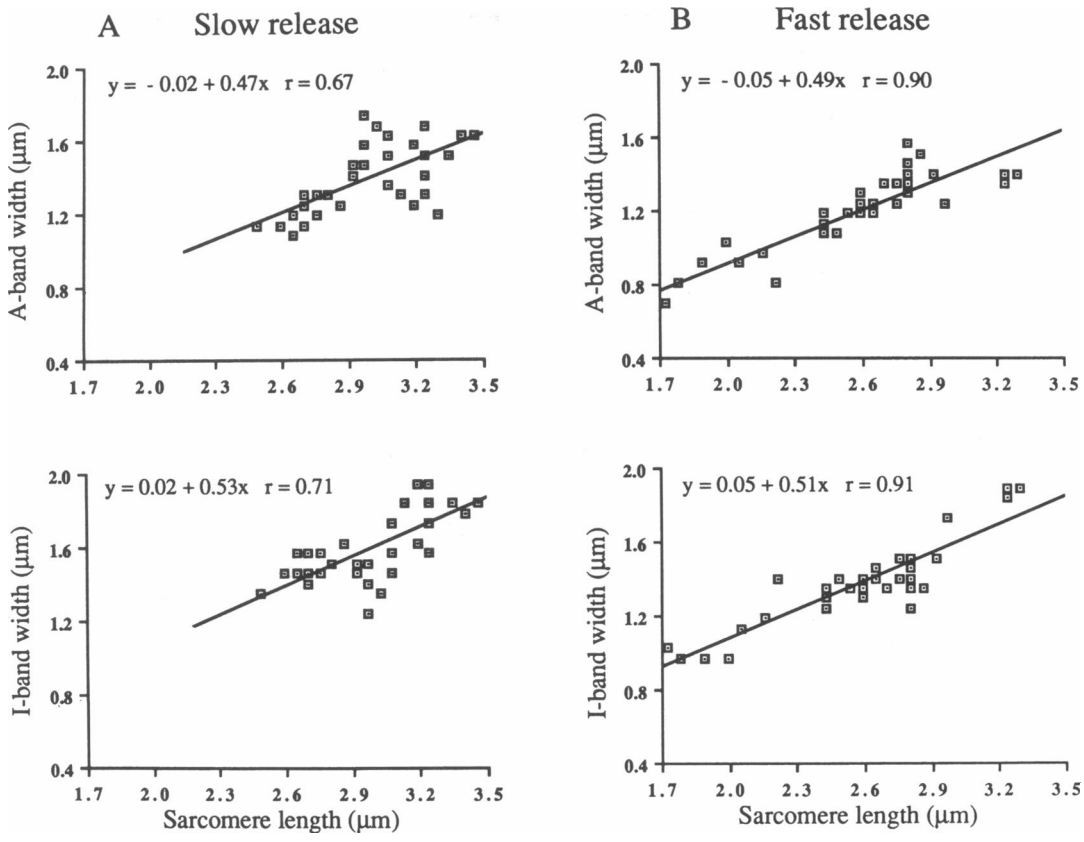


FIGURE 6 Data obtained during contraction with fiber shortening of 0.1 lengths per second (*A*); and 0.5 lengths per second (*B*). Regression lines shown. Number of data points: (*A*) 53; (*B*) 38. Several of the squares are composites of multiple data points.

As a step toward checking for any such optical effects we reanalyzed our data using both 70% and 30% criteria to supplement the standard 50% criterion. Results obtained using these rather extreme criteria are shown in Fig. 7. Although quantitative differences arise, substantial A-band shortening is found independent of the choice of criterion. This diminishes the likelihood that the A-band shortening arose out of secondary optical effects, though it does not completely rule out this possibility.

## Effect of translation

Another possible source of error is specimen translation during the flash exposure. This may blur the striation pattern, thereby resulting in potentially mismeasured band widths. The problem occurs in both passive release and in active release, because the moving end of the fiber is continuously translating; but it may be particularly severe in the activated release, as local motion is more unpredictable. In theory, this might be a source of artifactual A-band shortening.

To check this, we took advantage of a quirk in the optical recording system. The full field of the video image comprises the sum of two frames, each taken 1/60 second apart. Because the xenon strobe flashed each 1/60 second, we were able to compare striation patterns recorded at two closely spaced instants, 1/60 second apart, and thereby assess the amount of translation that took place during this interval.

This procedure was carried out on five contracting fibers. We compared the locations of the A-I junctions in successive frame pairs. In no instance was the shift greater than one pixel spacing, which corresponds to 0.054 $\mu$m in the fiber. Thus, the amount of translation that occurs within the exposure window was too small to have been responsible for the observed changes of band width.

## Effect of image quality

Whereas images obtained from relaxed, moderately stretched fibers were of reasonable quality (e.g., Fig. 2), those obtained from actively shortened fibers were usually poorer: striation nonuniformity increased, and skew was often more severe. The question arises whether analysis of such data is reliable.

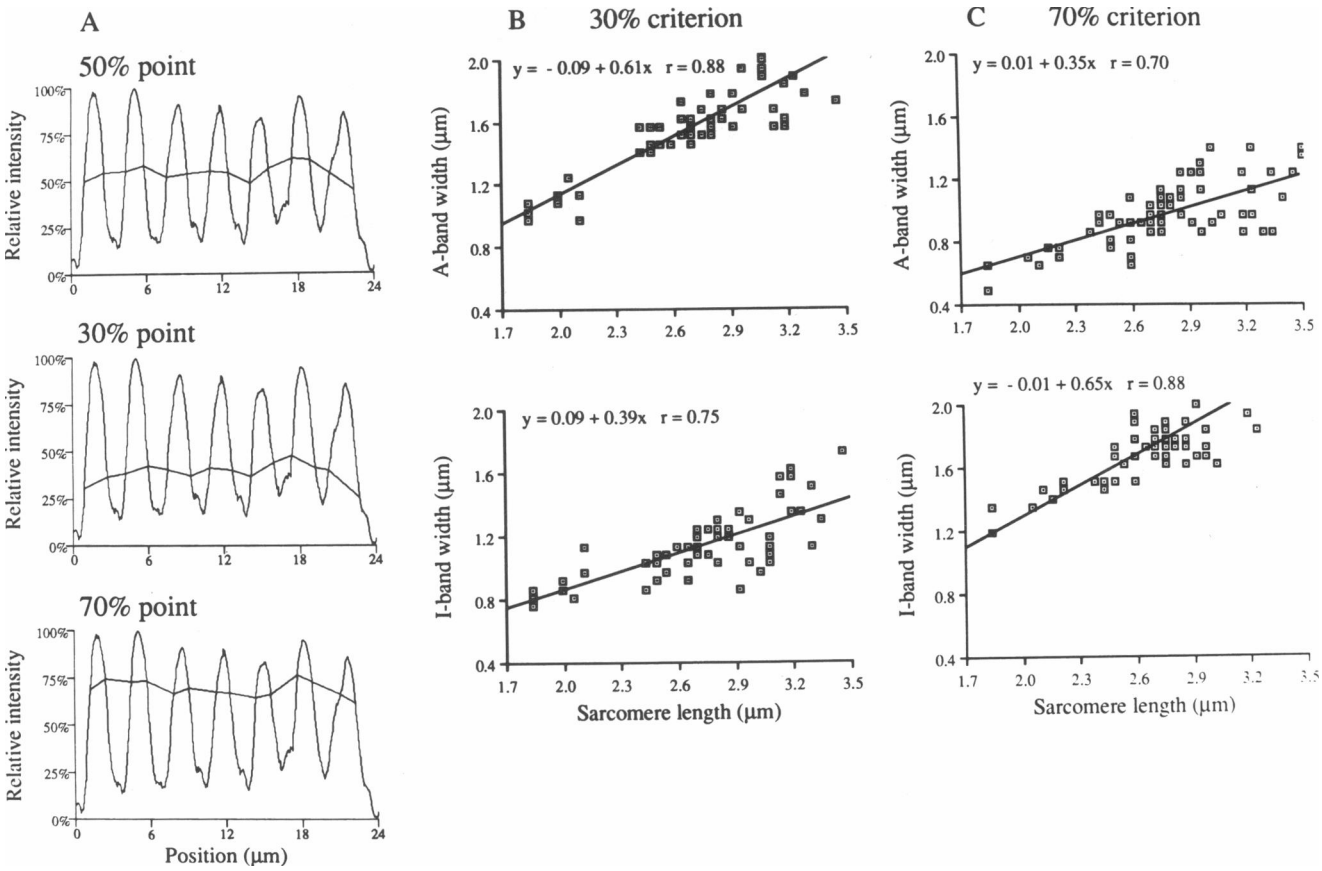


FIGURE 7 Influence of A/I boundary criterion on band dimensions. (*A*) Representative densitometry trace from relaxed image, with boundary designations based on 50% (standard) criterion; 30%; and 70%. Sarcomere length, ~3.2 μm. (*B* and *C*) Randomly chosen subset of data points of Fig. 4, reanalyzed using 30% criterion (*B*) and 70% criterion (*C*). Number of data points: (*B*) 71; (*C*) 74. Several of the squares represent multiple data points.

A representative image of an actively shortened sarcomere is shown in Fig. 8 (*upper left*). The sarcomeres in this field had shortened from 3.2 μm to the ~2.0 μm shown in the figure. The image is fairly poor. Intensity variation across the field is severe, and correction by background ratioing did not fully correct this variation. Skewing is nonuniform, and band widths appear to vary along the field.

Deskewed images obtained from upper and lower regions of the image are shown beneath. (The size of these regions is typical of those selected for deskew.) Deskewing is moderately effective, with residual skew remaining, particularly in the righthand portion of each image.

A densitometer trace taken from the lower of the two regions is shown below. A- and I-band widths obtained using the 50% criterion fall within the range shown in Fig. 4, scatter in band widths and sarcomere lengths being greater than in the superior images from relaxed fibers. The increased inhomogeneity is corroborated by EM results, below. (Such inhomogeneity adds uncertainty to the graphs of Figs. 4, 6, and 7, particularly at short sarcomere lengths.) A-Band widths measured using the 70% criterion (*right*) are larger than those obtained with the 50% criterion, while 30% values are lower. These criterion-based shifts are similar in magnitude to those obtained from the relaxed fibers (compare Fig. 7). In other words, poorer images notwithstanding, data obtained from activated fibers at short sarcomere length appear to yield reasonable data.

## Influence of de-skewing algorithm

In theory, band dimensions are most reliably obtained by analyzing single-line scans across the image. However, such scans cover an extremely small width—on the order of the spacing between filaments—and are therefore noisy. By averaging across the image, the signal-to-noise ratio is increased. Although the increased signal-to-noise

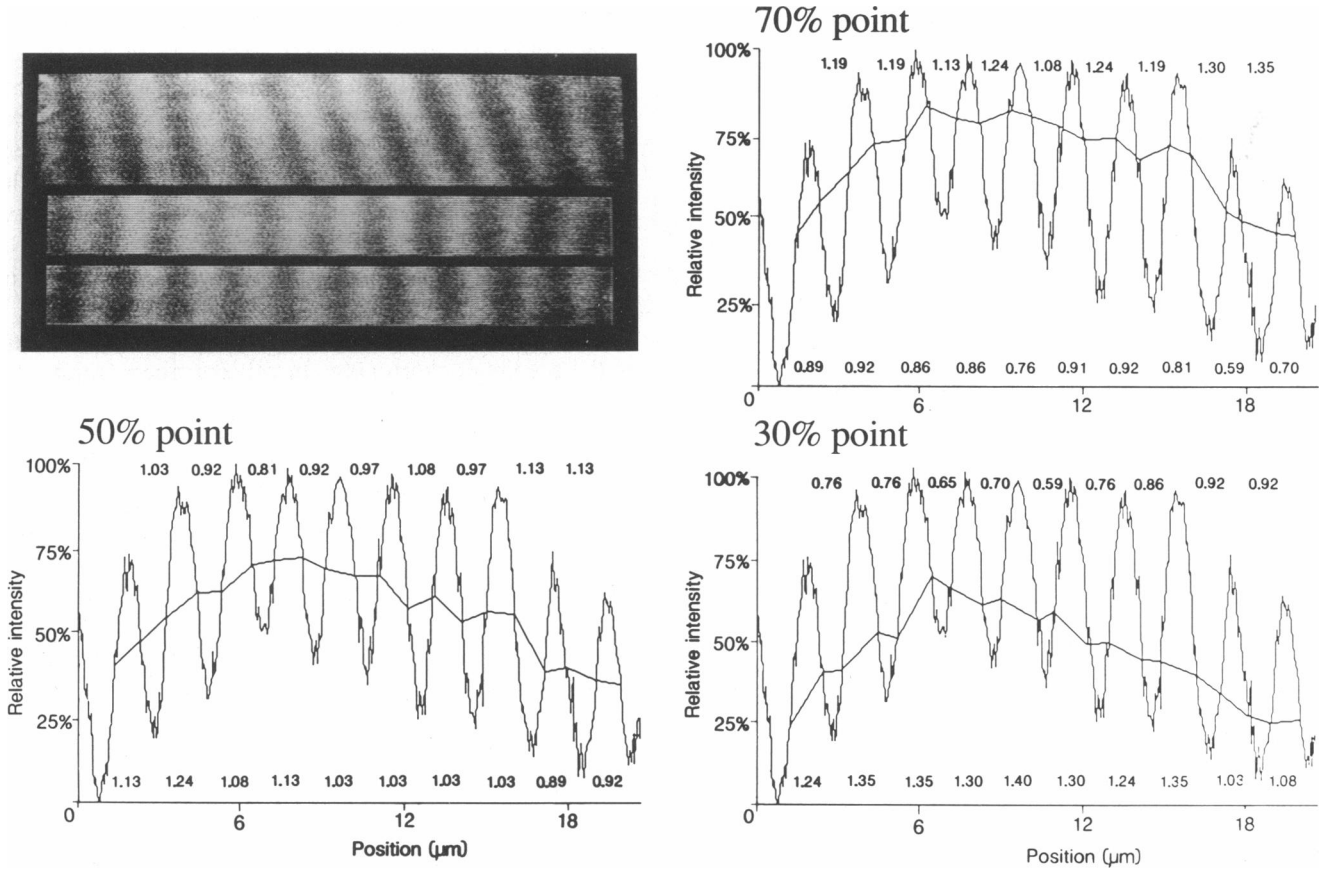


FIGURE 8 Analysis of an image obtained from a highly shortened fiber. Original image, corrected only for intensity variation, is shown at upper left. De-skewed images obtained from upper and lower halves of original image are shown beneath it. Densitometer trace for lower image is presented, with analysis based on 50% criterion (*lower left*), and 70% and 30% criteria (*upper right*). Numbers above and below each trace refer to individual I- and A-band widths, respectively.

ratio should lead to more definitive results, the required band deskewing introduces potential uncertainties that need to be dealt with.

To test whether the deskewing algorithm introduced unsuspected error into the analysis, an arbitrary fraction of images was analyzed without skew reduction or processing of any kind. The image was displayed, and a cursor was set at the apparent A/I boundaries along a string of consecutive sarcomeres. The computer then calculated mean A- and I-band widths for the string. The process was repeated at several locations on each image, and the grand means were obtained. These values comprised a single pair of data points for that image.

The results of this analysis are presented in Fig. 9. All data points are for activated, shortening sarcomeres. Although the data are scattered, and the *r*-values relatively low, the regression lines are indistinguishable from those obtained when the deskewing algorithm was used (Fig. 4).

## Chemically fixed specimens

As an independent test of A-band shortening, we carried out a series of parallel experiments in which thick filament lengths could be measured directly. Specimens were fixed at rest or immediately after activated shortening. Although specimens were fixed in two ways, we found the mercuric chloride fixation—though purportedly instantaneous—gave relatively poor images. Individual thick filaments could not be discerned, and we were therefore uncertain about potential artifacts. Thus, we relied primarily on glutaraldehyde-fixed specimens.

Fig. 10 shows representative images of glutaraldehyde-fixed specimens, prepared at rest (*top*) and after activated shortening (*bottom*). Several differences are obvious. First, the images of the relaxed sarcomere is more regular; Z-lines are relatively straight and filaments are well discerned. The activated specimen, by contrast, is more irregular, with Z-lines more ragged and running

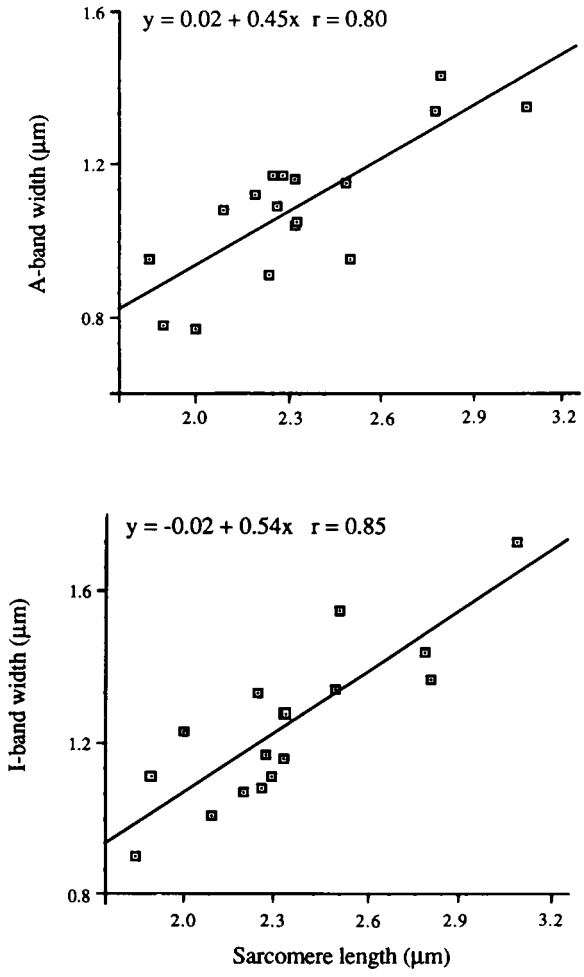


FIGURE 9 Analysis of changes of band widths during active sarcomere shortening using an alternative analytical method. De-skewing algorithms were not applied. Data were obtained from a fraction of images used to construct Fig. 4 *B*.

sinuously across the myofibril. No fine periodicity is apparent. Image character is somewhat "grainier" than in the unactivated sarcomere, and spaces between myofibrils are wider, possibly as a result of water exclusion from within the contracting myofibril. Thin filament tips can be recognized in the relaxed specimens, but in contracted specimens, graininess and Z-line skew usually precluded identification of this boundary. Of all activated images, the boundary was clearest in Fig. 10, which hints of substantially shortened thin filaments—similar to earlier observations by Samosudova and Frank (1971) in experiments similar to ours. Thick filaments, by contrast, were well identified in either state; generally, they could be followed along their entire length, precluding serious tilt artifacts and consequent foreshortening. The difference of thick filament length in the two panels is clear.

Fig. 11 summarizes the thick filament lengths measured from six contracted specimens, plus a control (unstimulated). Measurements were carried out as follows: Large photographic prints containing a field of some 20–30 myofibrillar sarcomeres were examined, one or two prints per fiber. Eight sarcomeres from each print were chosen randomly, and thick filaments measured. The eight values were then averaged, thereby giving one data point. The standard deviation reflects the degree of variability of thick filament length within the print, as well as the uncertainty in the measurement.

The figure shows substantial thick filament shortening with sarcomere shortening. In relaxed fibers, thick filament length was 1.61 μm, extraordinarily uniform over the field. The maximum thick filament shortening we observed was ~0.35 μm, but more often we observed 0.2–0.3 μm. Occasional regions showed stretched sarcomeres; in these regions thick filament lengths were intermediate between those in the relaxed and shortened sarcomeres. Results obtained with mercuric chloride fixative also showed consistent thick filament shortening, but image quality was sufficiently poor that we felt the results were not trustworthy.

## DISCUSSION

The major finding of this study is that shortening of the activated sarcomere is accompanied by modest but definite shortening of the A-band. Parallel studies carried out with electron microscopy revealed thick filament shortening of comparable magnitude.

### Sources of error

We considered several potential sources of artifact that might have given rise to the decrease of A-band width observed in these experiments.

The major concern in any optical micrographic study is whether an observed dimensional change is a reflection of some molecular event, or arises from the microscope's limited resolution. In their pioneering work on the subject, Huxley and Niedergerke (1958) were much concerned with this question and were inclined to attribute their observed A-band shortening to just this factor. Thus, their observation that the I-band never decreased to below 0.7–0.75 μm instead of to zero, was considered due to the microscope's inability to resolve increasingly narrow bands, especially when bisected by an optically dense Z-line. (With I-bands remaining above 0.7 μm and sarcomeres shortening to as low as 1.5 μm, the A-band apparently shortened to as low as 0.8 μm.)

Our experiments were carried out using equipment with higher resolution. Thus, if an artifactual decrease of A-band width occurred, it would be anticipated to have

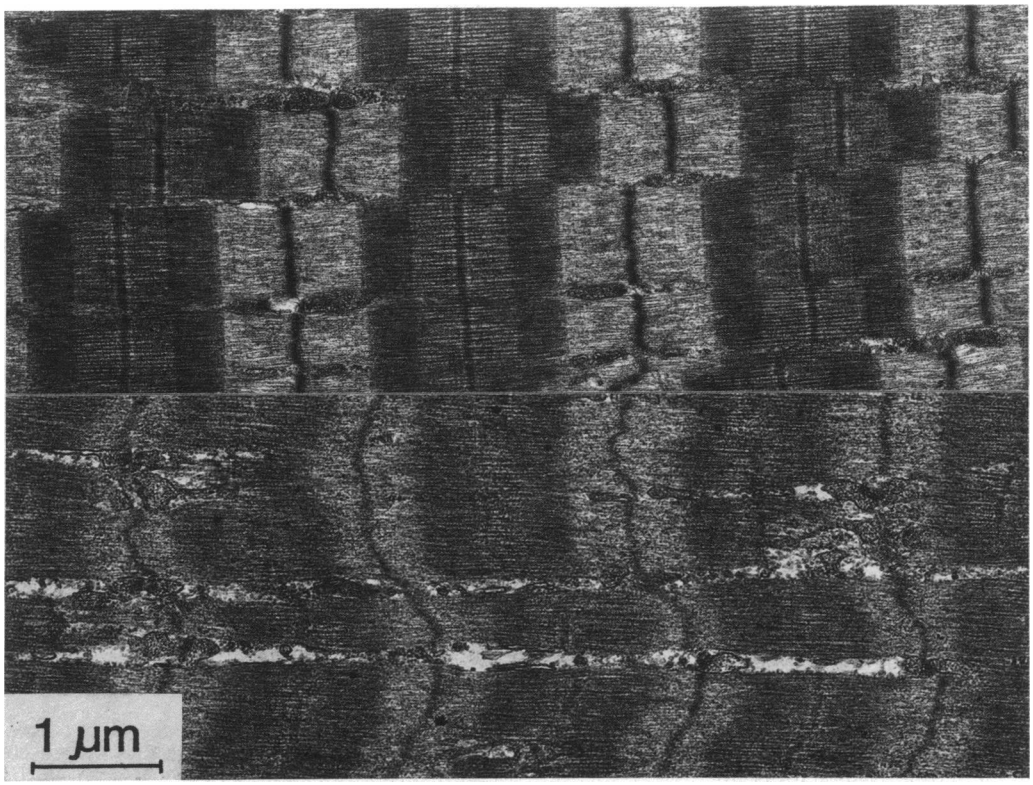


FIGURE 10 Electron micrographs of samples fixed at rest (*top*) and immediately after activated isotonic shortening (*bottom*). Note difference of thick filament length.

set in at sarcomere lengths shorter than the 2.3 μm found in the Huxley-Niedergerke study. In fact, the A-band shortening began at equal or longer sarcomere lengths. Nevertheless we carried out a series of control experiments to check for optically-induced A-band shortening:

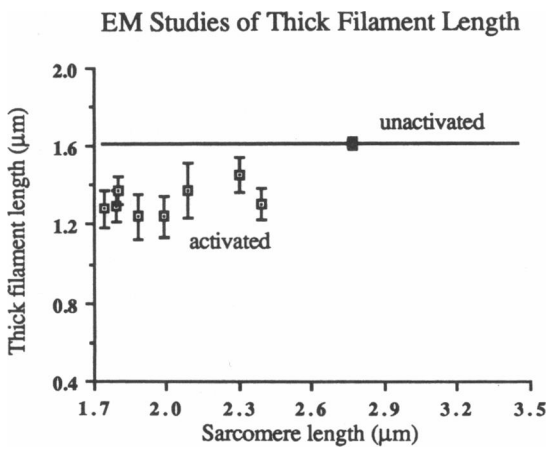


FIGURE 11 Summary of results obtained with glutaraldehyde fixation. See text for experimental details.

the fiber was released at the same speed with and without stimulation; only when the fiber was stimulated did the substantial A-band shortening occur. Thus, A-band shortening in these experiments did not appear to arise from limitations of optical resolution.

Another possibility is that the diminution of A-band width arises because of the analytical procedures used to measure A-band width. Like Huxley and Niedergerke, we "defined" the A-I boundary as the midpoint of the A/I intensity excursion, i.e., the 50% point. During active shortening many things may change: the bands may skew; the birefringence pattern along the sarcomere may change; the refractive index may change, etc. All of these factors limit confidence in the choice of boundary. Hence, we considered it prudent to see if comparable A-band shortening would occur with the adoption of different sets of criteria to define the width of that band. Even with rather extreme criteria, "30%" and "70%" instead of 50%, the conclusion we drew was the same: substantial A-band shortening.

Another possibility is that the A- and I-bands were somehow confused. Band reversal may sometimes occur with bright field or phase microscopy, with attendant ambiguity. But with polarization and interference micros-

copy, such ambiguities are not expected to arise (Huxley, 1977). Nevertheless, reversal might conceivably occur if large changes of birefringence of the A- or I-band took place upon activation. Were this the case, our conclusion would not be affected, because approximately equal shortening took place in both A- and I-bands.

Yet another possibility is that the A-band shortening arose out of unsuspected artifact attendant with image processing—especially de-skewing. De-skewing was implemented to permit averaging across the field, and therefore to ameliorate the effects of noise. We found that the extent of A-band shortening was similar whether measured with or without the de-skewing algorithm.

Finally, we checked the effects of specimen translation. With the short, small diameter fibers used here, we found that the amount of axial translation occurring during the 25 $\mu$s of exposure time was negligible relative to band dimensions; fuzzing of the A-I boundary is therefore negligible. Blurring might also be induced by translation along either of the two other axes, but again, substantial A-band shortening took place only if the specimen had been stimulated during the release; passively released specimens showed almost constant A-band width with an otherwise identical protocol. Thus, a translation-induced A-band shortening artifact seems unlikely.

## Comparison with previous work

The definitive work on the subject was carried out more than 30 years ago by Hanson and Huxley (1955) and by Huxley and Niedergerke (1954, 1958). The former is of limited relevance here because active contraction was examined only below resting length; nevertheless, a change of A-band width on the order of 0.15 $\mu$m was noted (text, Fig. 2). The Huxley/Niedergerke experiments are more relevant, as our experiments were largely patterned after those. Although those results are generally held to imply constancy of A-band width, close examination of their data reveals only minor differences with the observations reported here.

The Huxley and Niedergerke experiments were carried out at a time when resolution was limited by available equipment. Thus, the numerical aperture of the objective lens, together with the total magnification was stated (p. 405) to give a lateral resolution no better than 0.4 $\mu$m. An additional 0.1–0.2 $\mu$m of image degradation was estimated to have arisen from movement of the film of the rotating drum camera during the flash exposure. Further degradation will have occurred because of the large depth of field; under the conditions given, depth of field can be computed to be ~4 $\mu$m, so that even minor striation skew can be expected to have given rise to some blurring of striation boundaries. Thus, final resolution was probably no better than 0.6 $\mu$m. But additional degradation may have resulted from specimen translation. The semitendinosus fibers used in those experiments are several centimeters long (ten times the length of the toe fibers used here) and may translate considerably during release. Especially with relatively long flash duration (~100 $\mu$s, calculated from the information provided), specimen translation may have induced some blurring of the edges of the A- and I-bands. With such resolution limitations, striation patterns can be expected to appear "clean" but fine details will have been lost.

The present experiments ameliorate some of these limitations. With short fibers and brief flash duration, effects of blurring due to axial translation will be some 40 times less. The rotating drum camera has been replaced by a video camera. The high sensitivity of this camera, coupled with the high intensity of the xenon flash, permitted us to attain higher total magnification; this reduced depth of field from 4 to 0.4 $\mu$m. Finally, lenses with higher numerical aperture were used. Thus, resolution was considerably higher in these experiments. When measured using an edge object, resolution was 0.35 $\mu$m; when calculated using the standard Rayleigh criterion, the value was 0.27 $\mu$m.

Notwithstanding these technical differences, our results are quite similar to those obtained by Huxley and Niedergerke (1958). In unstimulated fibers, Huxley and Niedergerke found an A-band width of 1.4–1.5 $\mu$m. Our results are similar. The increase of sarcomere length with passive stretch was accounted for largely by an increase of I-band width, as found here; however, there was also a slight concomitant increase of A-band width: all nine of their graphs containing data between 2.0 and 3.0 $\mu$m sarcomere length (text, Fig. 7) show this. Again, these results are similar to what was found here.

Our results obtained with activated, shortening fibers differ only slightly. Huxley and Niedergerke present no graphs; only a single photographic sequence is shown (Fig. 3). The results are stated to be similar to those obtained during passive release: little or no change of A-band width was observed down to 2.4 $\mu$m, followed by a fall of A-band width with further shortening. (Initial sarcomere length was not stated.) Our data do not differ greatly: If the region above, say 2.6 $\mu$m is considered in isolation, the decrease of A-band width is hardly apparent (Fig. 4 *B*), and is not significantly different from the decrease of A-band width seen during passive shortening (compare Fig. 4 *A*). With further shortening, the fall of A-band width becomes more obvious and substantial. In the absence of any further quantitative data provided by the Huxley and Niedergerke study, it is difficult to ascertain whether the two sets of results differ at all.

In a sense, then, our observations confirm and extend those of Huxley and Niedergerke: little variation of A-band width with passive release or stretch; and definite

A-band shortening during active contraction. With the higher resolution of our system, there was some suggestion that the dimension of A-band width may have begun at, or just below, the starting sarcomere length (Fig. 4), but scatter of the data precluded definitive analysis. We also found approximately the same decrease of A-band width whether the load was small or moderate.

Apart from the Huxley and Niedergerke experiments, many investigators have considered the question of whether or not A-bands or thick filaments shorten during contraction. A comprehensive review of the subject has been published (Pollack, 1983), and while it is beyond the scope of this discussion to consider these papers in any detail, it is worth stating that A-band shortening or thick filament shortening has been observed by a surprisingly large number of investigators since the mid-fifties, particularly at intermediate and short sarcomere lengths. Thus, the observations of Huxley and Niedergerke, and our confirmation here, are not necessarily at odds with the bulk of the literature.

## Electron micrographic results

The EM studies were undertaken as an adjunct to the optical micrographic studies. We did not carry out enough experiments to derive any systematic relation between the amount of sarcomere shortening and the amount of thick filament shortening, as we did in the optical study. Our goal was limited to the determination of whether thick filaments were shorter in activated, shortened fibers than in unstimulated fibers.

Indeed, this is what was found. Thick filament length in unstimulated fibers was 1.61 $\mu$m, close to the commonly accepted value. Thick filament taper may account for the somewhat smaller width of the A-band measured optical microscopically both here and in the Huxley-Niedergerke study. In contrast to the 1.61 $\mu$m value found at rest, specimens fixed at the end of a period of activated shortening showed consistently shorter thick filaments, typically 1.3–1.4 $\mu$m but as low as 1.25 $\mu$m. This diminution, 0.2–0.3 $\mu$m, is slightly less than that measured by optical microscopy. On the other hand, it is the same as the value obtained if the optically measured A-band shortening is "corrected" for the small A-band shortening seen in the passively released fibers. Considering uncertainties inherent in both methodologies, any small quantitative difference is not surprising. The EM results essentially confirm the optical results.

As far as earlier EM work is concerned, the number of studies that address the question of thick filament length changes during isotonically loaded contraction from extended lengths is limited. In the work carried out by Hanson and Huxley (1955), this was not done. The most comprehensive EM study was carried out by Page and Huxley (1963), who were especially concerned about possible shrinkage artifact. Thus, several fixatives were used in a variety of experimental conditions, and the results implied little or no change of filament length during contraction. However, the data reported under the conditions of this study—shortening from extended sarcomere length under load—are scant (their Table 6, top). Only one sample is presented, and it is not clear whether the stated sarcomere length (3.3 $\mu$m) was the initial or final one, or how far the sarcomeres shortened during the contraction. Thus, it is uncertain whether any of the data reported in that study are relevant to the data presented here.

More recent isotonic work, carried out using the freeze-substitution method, has yielded conflicting conclusions. In work by Huxley et al. (1987), thick filament length changes were observed, but were assumed to have arisen out of preparation-induced shrinkage. After correction for shrinkage (based on the assumption that the reduced 143 Å A-band periodicity was a shrinkage artifact, not a physiological event), filament lengths were found to be similar to relaxed controls. In a second study (Edelmann, 1988) frog sartorius muscles contracting isotonically from long to intermediate sarcomere length were quick-frozen and freeze substituted. Thick filament shortening of ~15% was observed, similar to what was found here. However, filament-length determination was not the primary goal of that study, and few details were presented.

X-Ray diffraction studies bear only loosely on the issue. The constancy of spacing of layer lines and meridional reflections during contraction is generally taken as evidence that thick filaments do not shorten. However, such patterns are typically obtained during isometric contraction, not during contractions in which substantial sarcomere shortening has taken place. The one component of the pattern that has been studied during isotonic shortening is the 143 Å meridional reflection (Yagi and Matsubara, 1984; Matsubara and Yagi, 1985; Huxley et al., 1989). However, in the first two papers at least (no figures given in the third), sarcomere shortening was restricted to 7% or less. Thus, x-ray evidence relevant to the issue of what happens during the large shortenings considered here has apparently not yet been obtained.

## Implications

Present views on the mechanism of contraction imply that thick and thin filaments remain at constant length during all sarcomere-length changes in the physiological range. We have confirmed what many have found previously: in unactivated sarcomeres that are forcibly stretched or allowed to retract, thick filaments do not change length. In activated, shortening fibers, however, our results imply that thick filaments (or A-bands) may indeed shorten.

The amount of shortening found here was only 15–20%; the balance of the sarcomere-length change was absorbed by the I-band.

To explain the apparent change of filament length, we can envision three potential types of mechanism, *a priori:*

*Uniform shortening along the filament.* This mechanism seems least likely, because the x-ray diffraction experiments cited above show little or no shift of the 143 Å reflection, at least during small amounts of active sarcomere shortening.

*Cross-bridge disorder.* The polarization microscopic image is based on the specimen's birefringent character, and is therefore highly sensitive to structural disorder. The effect of cross-bridge disorder might be particularly pronounced at the filament's ends, which are tapered. Thus, A-band width may show a decrease that is unrelated to any change in filament-shaft length, but merely reflects cross-bridge disorder. An argument in favor of this interpretation is that the magnitude of the filament-length change obtained by electron microscopy, 0.2–0.3 μm, fits such a mechanism. Arguments against the interpretation are: (*a*) A-band shortening increased progressively with sarcomere shortening, whereas cross-bridge disorder would be expected to take force early upon activation. (*b*) The A-band shortening observed here with polarization microscopy is similar to that found by Huxley and Niedergerke using interference microscopy, a technique based on a different optical property. The similarity of results argues for a mechanism that is not specific to only one of the methods.

*Filament shortening one molecule at a time.* In this mechanism, the filament does not contract uniformly, but shortens by a molecule (or several) at a time, in sequence. A recruitment mechanism of this sort appears provisionally consistent with the results of x-ray diffraction mentioned above: unshortened molecules contribute as they did at rest, conferring constancy on the 143 Å repeat; shortened molecules no longer contribute, and therefore cause a progressive decrease of intensity. Both of these features are observed (Yagi and Matsubara, 1984; Matsubara and Yagi, 1985; Huxley et al., 1989).

Whether a decrease of thick filament length might be a primary (force-generating) process or a secondary process is not yet clear. The large A-band shortening often seen at short sarcomere lengths (cf. Pollack, 1983) is generally attributed to compression by the Z-line—presumably a passive phenomenon. However, the decrease of thick filament length found here begins at longer sarcomere lengths, and could therefore be actively based. Active thick filament shortening has been implicated in *Limulus* telson muscle (cf. Dewey et al., 1984 for review). The possibility that thick filament shortening may be involved in the contractile mechanism needs to be considered. This is not a new idea. Before the mid-fifties, such shortening was favored as the primary contractile mechanism.

*Received for publication 24 October 1988 and in final form 2 January 1990.*

## REFERENCES


Brown, L. M., and L. Hill. 1982. Mercuric chloride in alcohol and chloroform used as a rapidly acting fixative for contracting muscle fibres. *J. Microsc.* 125:319–336.

Dewey, M. M., P. Brink, D. E. Colflesh, B. Gaylinn, S.-F. Fan, and F. Anapol. 1984. *Limulus* striated muscle provides an unusual model for muscle contraction. *In* Contractile Mechanisms in Muscle. G. H. Pollack and H. Sugi, editors. Plenum Press, New York. 67–87.

Eberstein, A., and A. Rosenfalck. 1963. Birefringence of isolated muscle fibres in twitch and tetanus. *Acta Physiol. Scand.* 57:144–166.

Edelmann, L. 1988. The cell water problem posed by electron microscopic studies of ion binding in muscle. *Scanning Electron Microsc.* 2:851–865.

Edman, K. A. P. 1975. Mechanical deactivation induced by active shortening in isolated muscle fibres of the frog. *J. Physiol. (Lond.).* 246:255–275.

Granzier, H. L. M., and G. H. Pollack. 1985. Stepwise shortening in unstimulated frog skeletal muscle fibres. *J. Physiol. (Lond.).* 362:173–188.

Hanson, J., and H. E. Huxley. 1955. The structural basis of contraction in striated muscle. *Symp. Soc. Exp. Biol.* 9:228–264.

Huxley, A. F. 1977. Looking back on muscle. *In* Pursuit of Nature. Cambridge University Press, Cambridge, UK. 23–64.

Huxley, A. F., and R. Niedergerke. 1954. Structural changes in muscle during contraction. *Nature (Lond.).* 173:971–973.

Huxley, A. F., and R. Niedergerke. 1958. Measurement of the striations of isolated muscle fibers with the interference microscope. *J. Physiol. (Lond.).* 144:403–425.

Huxley, H. E., A. R. Faruqi, and S. Whytock. 1987. Correlation between x-ray diffraction studies on contracting muscle and electron microscope observations using rapid freezing techniques. *Biophys. J.* 51:5a. (Abstr.)

Huxley, H. E., R. M. Simmons, and A. R. Faruqi. 1989. Time course of spacing change of 143A meridional crossbridge relection during rapid shortening. *Biophys. J.* 55:12a. (Abstr.)

Matsubara, I., and N. Yagi. 1985. Movements of cross-bridges during and after length changes in active frog skeletal muscle. *J. Physiol. (Lond.).* 361:151–163.

Page, S., and H. E. Huxley. 1963. Filament lengths in striated muscle. *J. Cell Biol.* 19:369–391.

Periasamy, A., D. N. Holdren, W. C. Everts, and G. H. Pollack. 1985. Image processing of muscle striations. *Proc. Annu. Conf. Engin. Med. Biol.* 7:971–975.

Pollack, G. H. 1983. The cross-bridge theory. *Physiol. Rev.* 63:1049–1113.

Samosudova, N. V., and G. M. Frank. 1973. Change in the ultrastructure of the contractile apparatus of cross-striated muscle with the tonic type of contraction. *Biofizika.* 16:244–253.

Yagi, N., and I. Matsubara. 1984. Cross-bridge movements during a slow length change of active muscle. *Biophys. J.* 45:611–614.